PHYSICAL REVIEW C VOLUME 18, NUMBER 5 NOVEMBER 1978

Elastic pion scattering from ^{6,7}Li and ^{12,13}C†

S. A. Dytman, J. F. Amann,* P. D. Barnes, J. N. Craig,‡ K. G. R. Doss, R. A. Eisenstein, J. D. Sherman,* and W. R. Wharton
Carnegie-Mellon University, Pittsburgh, Pennsylvania 15213

G. R. Burleson and S. L. Verbeck§
New Mexico State University, Las Cruces, New Mexico 88003

R. J. Peterson
University of Colorado, Boulder, Colorado 80309

H. A. Thiessen
Los Alamos Scientific Laboratory, Los Alamos, New Mexico 87545
(Received 3 April 1978)

Elastic scattering of 50 MeV π^+ projectiles from targets of ^{6,7}Li and ^{12,13}C has been studied. Effects due to isotopic differences between targets are clearly visible in the data. The results are compared to three model descriptions for the cross section ratios for isotope pairs; in the case of ^{12}C-^{13}C a simple core-plus-valence-neutron model works well for ^{13}C if the core (^{12}C) potential describes observed ^{12}C elastic scattering. Such a model does not work for the ^{6}Li-^{7}Li ratio due to improper treatment of the scattering process and the quadrupole moments of the Li ground states.

[NUCLEAR REACTIONS Elastic scattering of 50 MeV π^+ from enriched ^{6}Li, ^{7}Li, ^{12}C, and ^{13}C. Angular distributions: $30° \leq \theta_L \leq 145°$. Optical model analysis of differences in scattering due to isotopic effects.]

I. INTRODUCTION

It has been known for some time now that elastic low-energy pion-nucleus scattering exhibits large and interesting differences between experiment and simple theoretical predictions.[1-3] These differences arise presumably because of the fact that the elementary πN (3,3) resonance is not so pervasive at these energies, so that the π has a longer mean free path in nuclear matter. Thus, effects due to the nuclear medium enter the problem at the outset, making the problem more complicated than a simple surface absorption mechanism. Recent calculations[4-7] which include nuclear medium effects have narrowed the differences with experiment and a somewhat clearer picture of this important process is beginning to emerge.

One of the main reasons that π-nucleus physics is of interest is the hope that we will be able to construct a given π-nucleus process (e.g., elastic scattering) from the basic π-nucleon amplitude and a suitable many-body theory. At energies below ~300 MeV, the basic πN amplitude[8] contains the usual s- and p-wave terms and a term responsible for nucleon spin flip. Each of these terms contains an isoscalar and isovector part, making six terms in all. In appropriate circumstances, all of them will manifest themselves in π-nucleus elastic scattering.

Until now, all nuclei studied, with the exception of ^{3}He (Ref. 9), have been even-even nuclei with zero ground state spin. For these targets, effects due to the nucleon spin-flip term will average to zero when scattering from the whole nucleus is calculated. In the case of self-conjugate even-even targets only the isoscalar part of the potential will be accessible, the isovector piece entering when $N \neq Z$ isotopes are studied. Information about the isospin structure of the non-spin-flip terms is thus potentially available from experiments already done.[1,3,10] However, no information directly pertaining to the spin-flip term is currently available.

A straightforward way of studying this issue is to perform elastic scattering from even-odd nuclei, hoping to describe the process as scattering from a core-plus-single-valence nucleon. The extent to which the extra nucleon can be described via the free π-N interaction would be a measure of the presence of nuclear matter, and would provide information regarding the effective π-N interaction in its presence.

As a first step in addressing this problem, we have studied elastic π^+ scattering at $T_\pi \sim 50$ MeV

from the isotope pairs ^{6,7}Li and ^{12,13}C. The experimental details are discussed in Sec. II, the theoretical analysis in Sec. III, and the conclusions in Sec. IV.

II. EXPERIMENT

The experimental work was performed on the EPICS channel at LAMPF under experimental conditions close to those reported in Ref. 2. The targets used were isotopically enriched slabs of material (see Table I) ranging in thickness from 150 mg/cm^2 for ^{7}Li to 926 mg/cm^2 for ^{12}C. The lithium targets were prepared by the Oak Ridge National Laboratory, while the ^{13}C target was fabricated at LASL using material obtained from the Mound Laboratories of the Monsanto Corporation.

Because of the large beam spot available at EPICS, each pair of isotopes was run simultaneously, with each target occupying ~48% of the beam area. The targets, mounted on a common frame, were separated from each other by 1 cm in the vertical (dispersion) direction and scattered pions from each were resolved spatially using three helical delay line proportional chambers.[2] The scattered pions were stopped, identified and their energy determined in the dual crystal intrinsic Ge spectrometer described earlier.[2,11] Figure 1 shows a vertical target projection of events identified as π^+; the 1 cm gap is clearly visible.

Halfway through each run the targets were vertically exchanged and rotated 180° so that all targets would be run at the same mean pion energy and so that systematic errors would be minimized. As in Ref. 2, the runs were normalized by comparing to πp differential cross sections[12] and using a set of ion chambers for angle-to-angle normalization.

For the Li and ^{13}C runs contaminant events had to be removed from each spectrum. The Li targets were each protected from oxidation by polyethylene bags which contributed a ^{12}C contaminant near the elastic peak of interest. The ^{7}Li target had the additional problem of an unresolved inelastic peak

TABLE I. Information pertaining to the targets used in the experiment.

Target	Thickness (mg/cm^2)	Purity (%)	Principal contaminants
^{6}Li	616	96	^{7}Li (4%)
^{7}Li	151	100	...
^{12}C	926	99	^{13}C (1%)
^{13}C	640	83	^{12}C (16%)

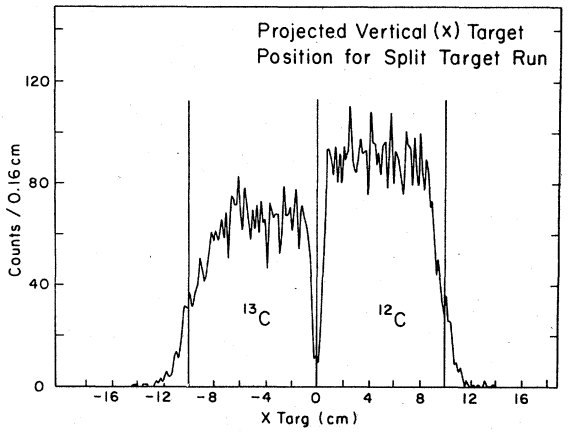

FIG. 1. The number of pions scattered from ^{12}C and ^{13}C as a function of target position in the momentum dispersion direction. The 1 cm gap between targets is clearly visible. Different areas for ^{12}C and ^{13}C reflect different target thicknesses.

($\frac{1}{2}^-$) at 0.478 MeV. The ^{13}C target contained a 16% admixture of ^{12}C due principally to the binder used in fabricating the target. In all cases the ^{12}C contaminants were removed by using their known percentage content in each target, the kinematic position, the cross section, and the elastic peak shape. The size of the ^{7}Li inelastic contaminant was estimated using the observed sum of counts in the ($\frac{7}{2}^-$) peak at 4.63 MeV and the ($\frac{7}{2}^-$)/($\frac{1}{2}^-$) cross section ratio measured to be approximately $\frac{2}{1}$ at 50 MeV in (p,p')[13] and 42 MeV in (α,α').[14] This correction is as large as 16% at 145° and 120°, 10% at 110°, and 8% at 100°. At more forward angles there is no sign of the 4.5 MeV level and therefore no correction was made to the elastic peak. This is consistent with previous (π,π') measurements at 50 MeV[2] which indicate a sharp falloff of inelastic cross section with decreasing scattering angle. Figures 2 and 3 show the energy spectra obtained for ^{7}Li at 120° and ^{13}C at 90°, respectively; these are rather typical of the results at other angles.

For comparison to theory, the angular distributions and the ratios of the cross sections for A and $A+1$ targets were used. The ratio in the center of mass frame is given by

$$R_{\text{c.m.}} = \frac{\sigma_A(\theta)}{\sigma_{A+1}(\theta)} = C\,\frac{J_A}{J_{A+1}}\left(\frac{A}{A+1}\right)\left(\frac{T_{A+1}}{T_A}\right)\left(\frac{N_A^U N_A^D}{N_{A+1}^U N_{A+1}^D}\right)^{1/2}. \quad (1)$$

Here C is a small correction (~1.01) for target misalignment, J_A and J_{A+1} are Jacobians for the

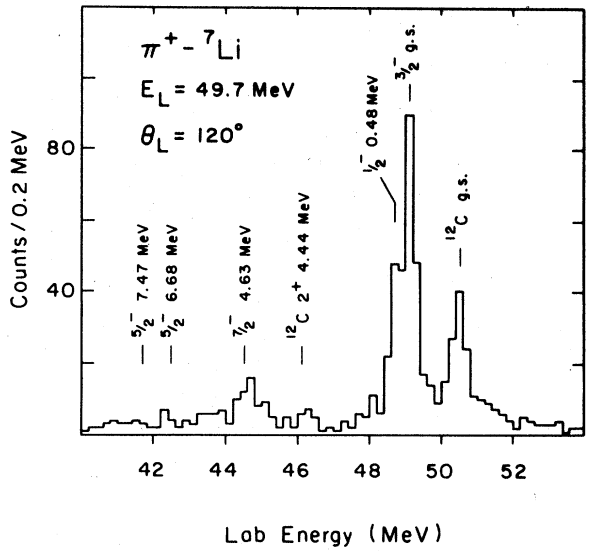

FIG. 2. The energy spectrum obtained for π^+scattering from the ^{7}Li target at θ_L 120°. This spectrum results after target projection and particle identification cuts have been made. Impurities have not been removed.

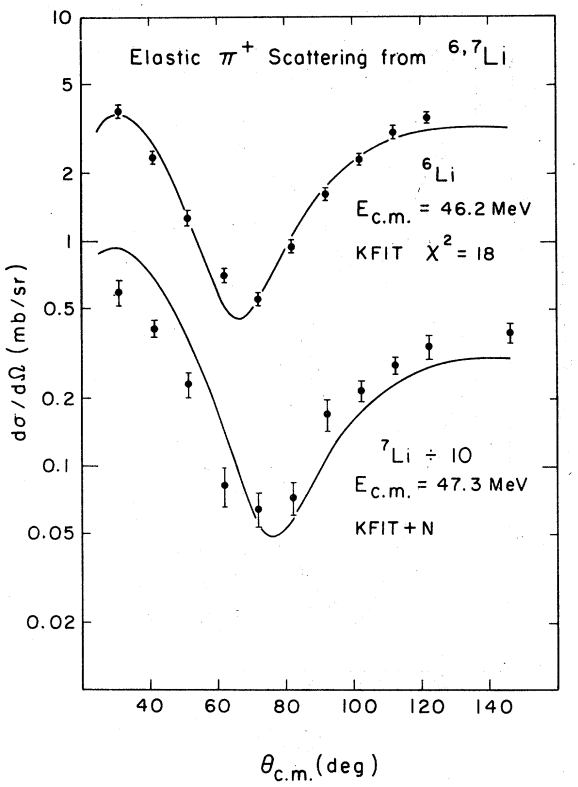

FIG. 4. The elastic scattering angular distributions for π^+scattering from ^{6}Li and ^{7}Li. The curve for ^{6}Li is obtained from a best-fit phenomenological Kisslinger potential whose parameters are given in the text. The curve for ^{7}Li is obtained from the KFIT + N prescription described in the text. The ^{7}Li data at θ_L = 100°, 110°, 120°, and 145° listed in Table II are shown here reduced by the percentages given in the text to account for the $(\frac{1}{2}^-)$ excitation at 0.478 MeV.

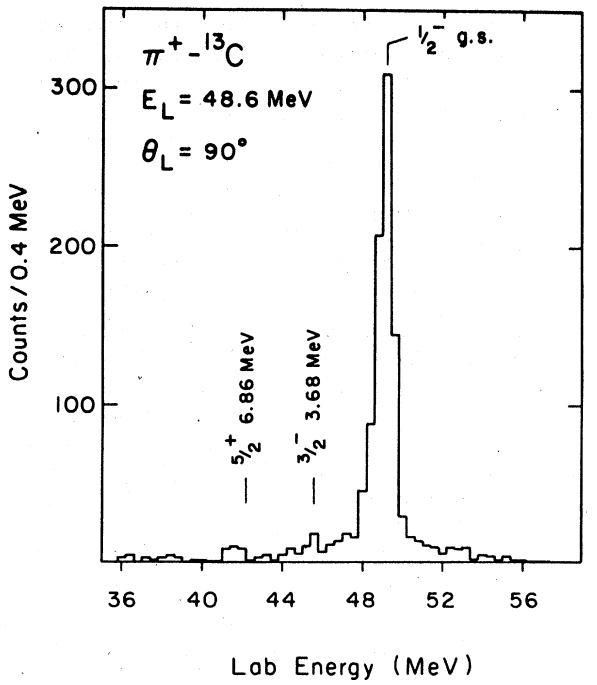

FIG. 3. The energy spectrum obtained for ^{13}C at θ_L = 90°; see Fig. 2 caption. The ^{12}C elastic peak is ~ 0.2 MeV lower than the ^{13}C elastic peak.

lab to c.m. transformation, T_A and T_{A+1} are target thicknesses, and, for example, N_A^U is the number of counts in the elastic peak corresponding to the A target in the up (U) position.

Figures 4 and 5 show the angular distributions for the Li and C targets obtained by summing the runs for the up and down target positions. Figure 5(a) also contains ^{12}C data obtained in Ref. 2 during earlier runs; comparison shows that the agreement is excellent. Figures 6 and 7, and Table II show the values obtained from Eq. (1) for the cross section ratios. The errors shown in Figs. 4 and 5 are statistical errors folded in quadrature with estimated errors due to dead time and gap corrections. The last two sources of error cancel out in the ratio determination, Eq. (1). An error of ±15% is assigned to the absolute normalization on scale

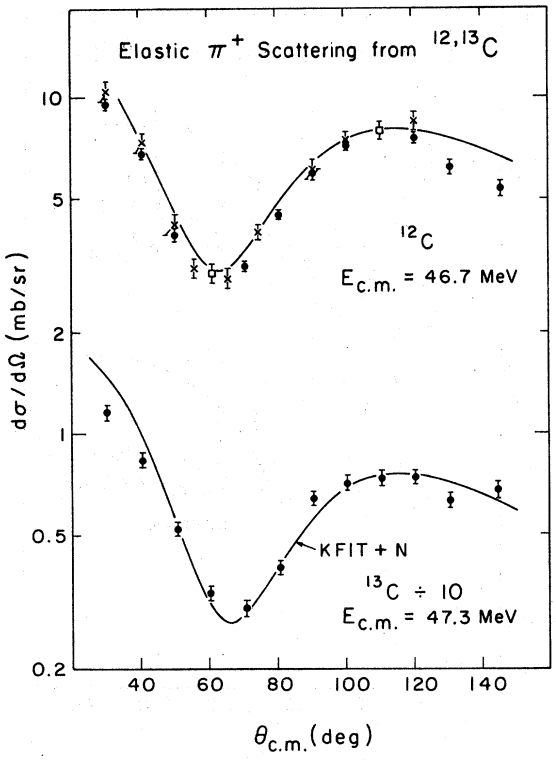

FIG. 5. The elastic scattering angular distributions for π^+scattering from ^{12}C and ^{13}C. The data obtained in this experiment are shown as dots, while the ^{12}C data of Rev. 2 are shown as crosses. Overlapping points are shown as boxes. The ^{12}C curve is from a best fit Kisslinger potential; see Ref. 2 and Table III. The ^{13}C curve is from the KFIT + N prescription described in the text.

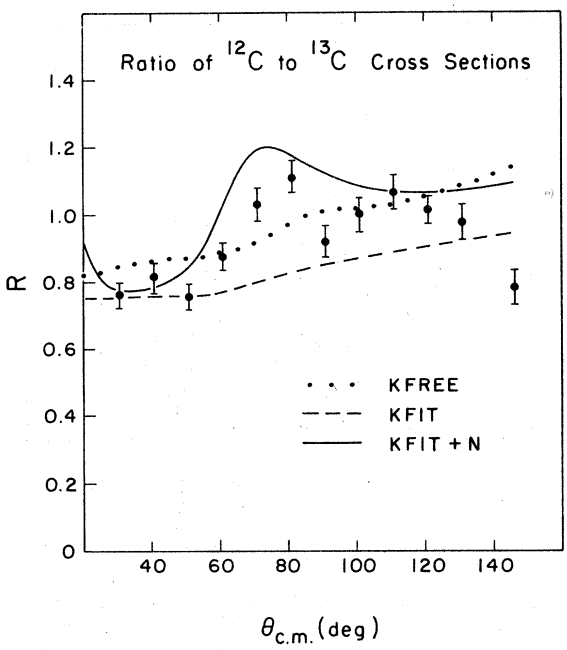

FIG. 6. The ratio R (^{12}C/^{13}C) of cross sections obtained from the experiment is compared to the calculations described in the text.

for the whole body of data, so that a renormalization would affect all cross sections equally. The individual angular distributions and the ratios are tabulated (with errors) in Table II.

TABLE II. A tabulation of all data taken in the experiment. All quantities are in the c.m. system. The scattering angle θ is in degrees and the elastic differential cross sections in columns 2, 3, 6, and 7 are in mb/sr. The measured cross section ratios are in columns 4 and 8. The last line gives the mean π^+ energy for each target. The ^{7}Li cross sections and the ^{6}Li/^{7}Li ratio at θ_L = 100°, 110°, 120°, and 145° have not been corrected for the ^{7}Li excitation at 0.478 MeV. See Figs. 4 and 7 and the text.

$\theta_{c.m.}$	^{6}Li	^{7}Li	R ($\frac{6}{7}$)	$\theta_{c.m.}$	^{12}C	^{13}C	R ($\frac{12}{13}$)
30.9	3.78 ± 0.24	5.92 ± 0.82	0.633 ± 0.085	30.4	9.57 ± 0.40	12.6 ± 0.61	0.763 ± 0.036
41.2	2.38 ± 0.14	4.05 ± 0.37	0.588 ± 0.052	40.6	6.86 ± 0.27	8.39 ± 0.41	0.814 ± 0.037
51.5	1.28 ± 0.09	2.30 ± 0.30	0.549 ± 0.067	50.7	3.92 ± 0.17	5.22 ± 0.26	0.755 ± 0.037
61.7	0.70 ± 0.05	0.81 ± 0.16	0.852 ± 0.171	60.8	2.95 ± 0.11	3.36 ± 0.17	0.875 ± 0.039
71.8	0.55 ± 0.04	0.64 ± 0.11	0.879 ± 0.150	70.8	3.17 ± 0.12	3.06 ± 0.16	1.032 ± 0.050
81.9	0.94 ± 0.06	0.72 ± 0.12	1.301 ± 0.201	81.0	4.48 ± 0.17	4.01 ± 0.18	1.114 ± 0.053
91.9	1.62 ± 0.10	1.69 ± 0.26	0.962 ± 0.143	91.0	5.93 ± 0.24	6.44 ± 0.32	0.920 ± 0.045
101.9	2.32 ± 0.13	2.31 ± 0.21	1.000 ± 0.078	101.0	7.25 ± 0.29	7.16 ± 0.37	1.011 ± 0.050
111.8	3.06 ± 0.16	3.04 ± 0.20	1.006 ± 0.045	110.8	7.86 ± 0.31	7.35 ± 0.38	1.068 ± 0.051
121.6	3.54 ± 0.21	3.92 ± 0.41	0.900 ± 0.089	120.8	7.62 ± 0.28	7.47 ± 0.33	1.018 ± 0.039
130	...	...	...	130.7	6.21 ± 0.28	6.37 ± 0.28	0.973 ± 0.049
145.9	...	4.45 ± 0.31	...	145.6	5.34 ± 0.27	6.84 ± 0.39	0.783 ± 0.052
Energy (MeV)	46.2	47.3			46.7	47.3	

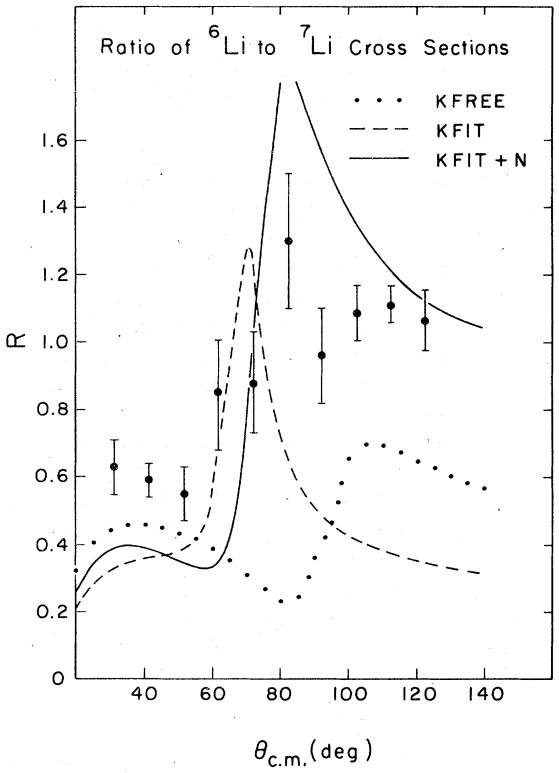

FIG. 7. The ratio R (^{6}Li/^{7}Li) of cross sections obtained from the experiment is compared to the calculations described in the text. The points at $\theta_L = 100°$, 110°, and 120° have been corrected for the ^{7}Li excitation at 0.478 MeV by dividing the entries in Table II by 0.92, 0.90, and 0.84, respectively.

III. THEORETICAL ANALYSIS

In accordance with the aims discussed above, we sought to analyze these data treating the odd-mass targets as a core-nucleus-plus-valence nucleon. The core was represented by a Kisslinger potential with best-fit optical parameters b_0 and b_1 taken from Ref. 2. The valence neutron was described by a free πn t matrix operating on a neutron matter density $\rho_n(r)$ calculated from shell model harmonic oscillator wave functions. The optical potential for the $A+1$ system is

$$2EV(\vec{r}) = [-Ak^2 b_0 \rho_c(\vec{r}) + Ab_1 \vec{\nabla}\cdot\rho_c\vec{\nabla}] + k^2 a_n \rho_n + b_n \vec{\nabla}\cdot\rho_n\vec{\nabla} + ic_n \vec{\sigma}\cdot\vec{\nabla}\times\rho_n\vec{\nabla}. \quad (2)$$

The last three terms represent the valence neutron; the coefficients a_n, b_n, and c_n were calculated from the phase shift determination of Rowe *et al.*[15] For π^+ projectiles the coefficients are

$$a_n = -\tfrac{1}{3}k_F(2\alpha^0_{11} + \alpha^0_{31}) = -3.66 - 0.858i,$$

$$b_n = \tfrac{1}{3}k_F(2\alpha^1_{11} + 4\alpha^1_{13} + \alpha^1_{31} + 2\alpha^1_{33}) = 3.01 + 0.438i,$$

$$c_n = -\tfrac{1}{3}k_F(2\alpha^1_{13} - 2\alpha_{11}{}^1 + \alpha_{33}{}^1 - \alpha_{31}{}^1) = -2.85 - 0.201i,$$

where the values have been calculated for $T_\pi = 48.6$ MeV. The quantities α are given by

$$\alpha^I_{2T,2J} = e^{i\delta_{2T,2J}} \sin\delta^I_{2T,2J}$$

and the kinematic factor k_F is $(4\pi s^2/m_N{}^2 p_0{}^3)$, with s the total c.m. energy, m_N the nucleon mass, and p_0 the c.m. π momentum.

The last term in Eq. (2) (involving the nucleon spinor σ) represents the possibility of nucleon spin flip and is the coordinate space expression of $i\vec{\sigma}\cdot\hat{n}\sin\theta$, with $\hat{n} = \vec{k}\times\vec{k}'/|\vec{k}\times\vec{k}'|$. The momenta $\vec{k}$ and $\vec{k}'$ represent the initial and final π-nucleus c.m. momenta and θ is the c.m. scattering angle.

One problem with the above expression is that the density ρ_n is generally not spherically symmetric. In addition, both the ^{6}Li and ^{12}C cores are deformed, and ^{6}Li and ^{7}Li have quadrupole moments in the ground state. (The ^{6}Li and ^{7}Li quadrupole moments are −0.0644 and −3.66 fm^2, respectively.[16]) Thus, in order to solve the problem generally, a coupling between partial waves should be included. Furthermore, the single-particle gradient operators should be in the pion-nucleon reference frame rather than the pion-nucleus frame as has been assumed. These improvements are beyond the scope of the present paper.

For the ^{12}C-^{13}C case an alternative approach is possible. We argue that effects such as core deformation and "angle transformation" (see e.g., Refs. 4–7) are accounted for by using the phenomenological parameters b_0 and b_1 in the potential. Further, the ^{12}C core is probably not polarized very much by the valence neutron since the low-lying spectrum of ^{13}C is fairly well described by a weak coupling shell model picture. The ground state is $\frac{1}{2}^-$ and has zero quadrupole moment. We assume that the valence neutron is a $1p_{1/2}$ orbital outside a ^{12}C core. The resulting neutron matter density is

$$\rho_n(\vec{r}) = |\phi_{nljm}|^2. \quad (3)$$

Here ϕ is the single-particle wave function for the neutron and in general is spherically nonsymmetric. Again a coupled channels analysis is required for correct analysis; instead we obtain a neutron matter density by averaging over m states *before* scattering

$$\rho_n(r) = \frac{1}{2j+1}\sum_{m\,\text{states}} |\phi_{nljm}|^2. \quad (4)$$

This expression is spherically symmetric and greatly simplifies our treatment although it in-

troduces some error into the analysis. For the $1p_{1/2}$ orbital we obtain

$$\rho_n(r) = \frac{2}{3}\left(\frac{\beta}{\pi}\right)^{3/2} x e^{-x} \tag{5}$$

with $x = \beta r^2$ and $\beta = m\omega/\hbar$, the oscillator length parameter. We use the usual shell model prescription[17] $\hbar\omega = 41/A^{1/3}$, giving $\beta = 0.42$ fm^{-2} for ^{13}C. The rms radius of the extra neutron is given by $\langle r_n^2\rangle^{1/2} = (5/2\beta)^{1/2}$.

When $\rho_n(r)$ is spherically symmetric, the spin-flip term in Eq. (2) can be reduced easily

$$c_n \vec{\sigma}\cdot\vec{\nabla}\times\rho_n\vec{\nabla}\psi - \frac{2c_n}{\hbar^2 r}\frac{d\rho_n}{dr}\vec{L}\cdot\vec{S}\psi = \frac{c_n}{r}\frac{d\rho_n}{dr}\begin{pmatrix} l \\ -l-1 \end{pmatrix}\psi \tag{6}$$

for the spin up and spin down cases. If ^{13}C is treated as an elementary particle of spin $S = \frac{1}{2}$, then the scattering of the spin zero pion from it can be treated in the usual way.[18] The computer code PIRK[19] was modified to do this.

The data on the ^{12}C-^{13}C comparison are compared to several predictions in Fig. 6. The quantity R is the ratio of the ^{12}C to ^{13}C elastic cross sections plotted against scattering angle. (See also Table II.) The deviation from unity is ~10%, or of order $1/A$, as expected. The "transition" from $R \sim 0.9$ to $R \sim 1.05$ occurs at 65°, the position of the s-p interference minima in the individual angular distributions. The minima in ^{13}C appears at a slightly more backward angle than in ^{12}C.

The simplest calculation one can do is to compute the individual cross sections using only the Kisslinger terms [bracketed part of Eq. (2)] but with A, b_0, b_1, and $\rho_c(r)$ appropriate for each nucleus. (See Table III.) Here b_0 and b_1 are calculated from free πN information[15] and depend on $N-Z$. Hence, the isovector interaction in ^{13}C will be crudely taken into account, while the necessary[1-3] s-wave repulsion is neglected as is the spin-flip term. This prediction is shown as a dotted curve in Fig. 6; apart from the transition region at ~75° the comparison to the data is not too bad. We refer later to this calculations as "KFREE." Since the ^{12}C and ^{13}C calculations individually do very poorly when compared to the angular distribution data, it is surprising that the ratios agree so well. Apparently the isovector and size effects, once included, do much to describe correctly the data, while core effects seem to cancel in the ratio.

Another calculation of interest is obtained by simply using the best-fit effective b_0 and b_1 from the ^{12}C experiment[2] but with $A = 13$ and ρ_c taken from electron scattering.[20] (See Table III.) This calculation has some deficiencies. Since the values of b_0 and b_1 are determined for a self-conjugate nucleus, they will overestimate the π^+-valence-neutron interaction. In addition, the spin-flip term is ignored and the electron scattering result measures only the proton distribution of ^{13}C. The result of the calculation is shown in Fig. 6 as a dashed curve; it is seen to reproduce the general rise of R as scattering angle increases, but its magnitude is ~10% too low. From this, one concludes again that the core effects are less important than the treatment of the valence neutron. We refer later to this calculation as "KFIT SCALED."

The third calculation shown in Fig. 6 is done using the potential formed from Eqs. (2), (4), (5), and (6). No adjustment of parameters was attempted. The result shown agrees well with the

TABLE III. The parameters used in the calculation of cross sections for the isotopes under study. The first three columns give the values of rms radius and p-shell Gaussian (harmonic oscillator) parameters determined in electron scattering (see Ref. 20). The ^{6}Li value for α is constrained to $(Z\text{-}2)/3$ and (a) is then obtained from the rms radius. The average lab energy for the scattering is given in column 5. The potential parameters b_0 and b_1 are phenomenological if enclosed by parentheses and from free πN information (Ref. 15) if not.

	$\langle r^2\rangle^{1/2}$ (fm)	a (fm)	α	E_L (MeV)	b_0	b_1
^{6}Li	2.56	1.89	0.333	48.9	$-1.050 + 0.672i$ $(-4.48 + 1.14i)$	$7.665 + 0.869i$ $(9.57 - 0.27i)$
^{7}Li	2.39	1.77	0.327	49.7	$(-0.388 + 0.691i)$	$7.016 + 0.832i$
^{12}C	2.46	1.65	1.25	48.1	$-1.054 + 0.678i$ $(-3.59 - 0.65i)$	$7.650 + 0.843i$ $(7.23 + 1.78i)$
^{13}C	2.44	1.64	1.40	48.6	$-0.689 + 0.688i$	$7.302 + 0.827i$

systematics of the data. The most important features of the calculation appear to be the explicit treatment of the isovector interaction and a valence neutron density which lies outside the core density. Arbitrary parameter adjustment would no doubt improve the fit but the physical significance of this is unclear. An obvious improvement would be to use a more realistic neutron wave function or perhaps a value of β in Eq. (5) which gives a more reasonable value for the rms radius of the valence neutron. A correct treatment of the quantum mechanical scattering process should be done as well. Nevertheless, it is encouraging that the simple picture presented here predicts most of the features of the data correctly. We refer later to this calculation as "KFIT+N."

Calculations were done using Eq. (2) with and without the spin-flip term. In all cases studied its effect is found to be small, changing the ^{13}C cross section by at most 1%.

The ^{6}Li-^{7}Li data present much more severe problems. The worst of these involve the permanent deformation of the ground states, each having a significant quadrupole moment and therefore spin ≥ 1. A correct calculation would thus include these quadrupole deformations in ρ_c and ρ_n and would need to consider scattering of the spin-zero pion from a spin-1 and spin-$\frac{3}{2}$ target. Neither of these can be done in the presently available codes. More fundamentally, it is not clear that a picture of ^{7}Li as $^{6}\mathrm{Li}+n$ is the most correct one. Other descriptions, such as $^{7}\mathrm{Li}=^{4}\mathrm{He}+^{3}\mathrm{H}$, should also be explored.

Figure 7 shows the experimental results for the ratio R of ^{6}Li to ^{7}Li cross sections as a function of scattering angle θ. As with C, the observed effect of the extra neutron is $\sim 1/A$, the ratio varying between ~0.6 and ~1.0. A transition is again seen to occur at $\theta \sim 65^\circ$ corresponding to the minimum in the individual cross sections. A KFREE calculation is also shown (dotted curve); it misses the data badly owing in part to the sharpness of the s-p interference minimum in the individual free πN calculations and the resulting large sensitivity to the difference in position of the minima. Also the minima in the actual data are much further forward than in the free πN case and much less sharp; these facts can be expected to exacerbate the disagreement of the KFREE result with the data.

A KFIT calculation can also be done provided that the ^{6}Li data are fitted first to a phenomenological Kisslinger model [the bracketed terms of Eq. (2) with adjusted b_0 and b_1]. Doing this yields for ^{6}Li the parameters $\mathrm{Re}b_0 = -4.48 \pm 3\%$, $\mathrm{Im}b_0 = 1.14 \pm 130\%$, $\mathrm{Re}b_1 = 9.57 \pm 2\%$, and $\mathrm{Im}b_1 = -0.27 \pm 750\%$. The fit was done using a p-shell Gaussian in PIRK[19] and constraining the rms radius to the electron scattering value[20] (2.56 fm). These fitted values differ substantially from the average set determined from 50 MeV π^+ scattering from several light nuclei,[2] although the real parts are again well determined and the imaginary parts poorly so. The latter effect may be due to the absence of diffraction effects in these processes: the (3,3) resonance is far removed from this energy region, and the form factor zero is inaccessible for these targets and momentum transfers. In view of the deformed nature and light mass of ^{6}Li the deviation from the average results of Ref. 2 is not surprising. The KFIT SCALED calculation is shown as a dashed curve in Fig. 7 and is also seen to do poorly compared to the data.

The last calculation shown in Fig. 7 is a modified KFIT+N, in which the spin-flip term is discarded and both nuclei are treated as spin-zero objects. The calculation thus only includes an isovector part calculated from free πN information and a distinct neutron distribution calculated from shell model wave functions as described above [Eq. (6)] with $\beta = 0.517$ fm^2. Apart from the sharp spike at $\theta \sim 75^\circ$, the basic trends of the data are reproduced. This may be completely spurious, or may indicate the necessity of including core effects as well as the isovector part of the π-nucleus interaction. An improvement on these results awaits a better theoretical calculation. The scattering formalism must be corrected and a better description of the nuclear structure of ^{7}Li used.

IV. SUMMARY AND CONCLUSIONS

This experiment has produced data which clearly show the effect of a single nucleon on elastic π scattering. The magnitude of the effect is of order $1/A$ as expected. In addition, the s-p interference minimum in the angular distribution for the $(A+1)$ nucleus is 5° further backward than in the (A) nucleus case. In the case of ^{13}C the ground state properties are such that a reasonably accurate treatment of the scattering process can be made by describing ^{13}C as a ^{12}C core plus a valence $1p_{1/2}$ shell model neutron. Three calculations (of increasing sophistication) are compared to the data and all reproduce the general features of the data. When describing the ratio of elastic scattering cross sections the effects of the core nucleus are found to be less important than a reasonable treatment of the extra nucleon. The best calculation relies on a separate π-neutron interaction potential in addition to the phenomenological core. Better data will be required to test the calculations more conclusively.

The ^{6}Li-^{7}Li data present more fundamental problems. The cross section ratio R (see Table II and Fig. 7) clearly shows the effect of the extra neutron and the magnitude again is of order $1/A$. However, attempts to describe the scattering process with the same calculation as used for ^{12}C and ^{13}C have not proved successful. This is due to two deficiences, the chief one being a failure to treat properly the ground state spin and deformation of the targets with a correct scattering formalism. One should also consider other descriptions of the ^{6}Li and ^{7}Li ground states, e.g., ^{7}Li as ^{4}He+^{3}H rather than ^{6}Li+n. A better description of our data requires a theory which incorporates such improvements.

We would like to thank the staff of the Clinton P. Anderson Meson Physics Facility for its cooperation in all phases of the experiment. We are greatly indebted to Mr. Robert Rohwer of LASL division WX-2 for fabricating the ^{13}C targets.

---

†Work supported in part by the U. S. Department of Energy.

*Present Address: Los Alamos Scientific Laboratory, Los Alamos, New Mexico 87545.

‡Present address: Science Applications, McClean, Virginia, 22101.

§Present address: W. H. B. Chan Co., Los Angeles, California.

[1]B. M. Preedom, in *Proceedings of the Seventh International Conference on High Energy Physics and Nuclear Structure, Zurich, 1977,* edited by M. P. Locher (Birkhauser, Basel, 1977) p. 119.

[2]S. A. Dytman, J. F. Amann, P. D. Barnes, J. N. Craig, K. G. R. Doss, R. A. Eisenstein, J. D. Sherman, W. R. Wharton, R. J. Peterson, G. R. Burleson, S. L. Verbeck, and H. A. Thiessen, Phys. Rev. Lett. 38, 1059 (1977) and 39, 53(E) (1977), and (unpublished).

[3]H. Dollard, K. L. Erdman, R. R. Johnson, M. R. Johnston, T. Masterson, and P. Walden, Phys. Lett. 63B, 416 (1976), and R. R. Johnson, T. Masterson, K. L. Erdman, A. W. Thomas, and R. H. Landau (unpublished).

[4]R. H. Landau and A. W. Thomas, Phys. Lett. 61B, 361 (1976), and (unpublished).

[5]N. J. DiGiacomo, A. S. Rosenthal, E. Rost, and D. Sparrow, Phys. Lett. 66B, 421 (1977).

[6]L. C. Liu and C. Shakin, Phys. Rev. C 16, 333 (1977); and (unpublished).

[7]K. Stricker, H. McManus, and J. Carr, (unpublished).

[8]D. Koltun, in *Advances in Nuclear Physics* (Plenum, New York, 1969) Vol. III p. 71.

[9]R. Landau, Ann. Phys. (N.Y.) 92, 205 (1975).

[10]E. Boschitz, in *Proceedings of the Seventh International Conference on High Energy Physics and Nuclear Structure, Zurich, 1977,* see Ref. 1, p. 133.

[11]J. F. Amann, P. D. Barnes, S. A. Dytman, N. Penkrot, A. C. Thompson, and R. H. Pehl, Nucl. Instrum. Methods 126, 193 (1975).

[12]P. Y. Bertin, B. Coupat, A. Hivernat, D. B. Isabelle, J. Duclos, A. Gerard, N. Miller, J. Morgenstern, J. Picard, P. Vernin, and R. Powers, Nucl. Phys. B106, 341 (1976).

[13]G. S. Mani, D. Jacques, and A. D. B. Dix, Nucl. Phys. A172, 166 (1971).

[14]R. J. Peterson, University of Washington Progress Report, 1964 (unpublished).

[15]G. Rowe, M. Salomon, and R. Landau, in *Contribution to the Seventh International Conference on High Energy Physics and Nuclear Structure, Zurich, 1977* (unpublished.

[16]E. Segrè, *Nuclei and Particles,* 2nd ed. (Benjamin, Reading, Massachusetts, 1977), pp. 276–277.

[17]A. de Shalit and H. Feshbach, *Theoretical Nuclear Physics* (Wiley, New York, 1974), p. 198.

[18]M. Melkanoff, T. Sawada, and J. Raynal, Methods Comput. Phys. 6, 1 (1966).

[19]R. A. Eisenstein and G. A. Miller, Comput. Phys. Commun. 8, 130 (1974).

[20]C. W. de Jager, H. DeVries, and C. DeVries, At. Data Nucl. Data Tables 14, 479 (1974).